Proceedings of the 9th U.S. National and 10th Canadian Conference on Earthquake Engineering
Compte Rendu de la 9ième Conférence Nationale Américaine et
10ième Conférence Canadienne de Génie Parasismique
July 25-29, 2010, Toronto, Ontario, Canada • Paper No 1119

SEISMIC ISOLATION USING SINGLE AND DUAL SHEAR HINGING OF TALL CANTILEVER WALL BUILDINGS SUBJECTED TO STRONG GROUND SHAKING

V. Calugaru[1] and M. Panagiotou[2]

ABSTRACT

This paper investigates numerically the effect of seismic isolation on the response of tall reinforced concrete cantilever wall buildings subjected to strong near-fault ground motions. Four 20-story cantilever reinforced concrete wall buildings are considered. The first building is designed to develop a single flexural plastic hinge at the base of the wall. The second building incorporates an isolation layer at its base. The third building incorporates an isolation layer at its base and at midheight, and the fourth building incorporates an isolation layer at its base and at seventy percent of the height. The four buildings are subjected to three strong near-fault ground motions. The nonlinear dynamic time history analysis of the buildings clearly shows that using isolators at one or two locations along the height of the buildings reduces significantly all engineering response parameters investigated, in comparison with those quantified for the building designed to develop a single flexural plastic hinge. The response is discussed in terms of displacements, forces, and accelerations.

Introduction

Reinforced concrete cantilever walls are commonly used as the main lateral force resisting elements in tall buildings in highly seismic regions (SEAONC 2007, Yang et al. 2008). These structures have to be designed for large demands, along the height of the buildings, if they are to be subjected to near-fault ground motions. In these tall buildings, near fault-ground motions can cause significant concurrent excitation of the first and higher modes of response (Krishnan 2007, Panagiotou and Restrepo 2009, Panagiotou et al. 2009).

Tall buildings are designed for reduced lateral forces, recognizing the possibility of developing nonlinear deformations in some parts of the structural system during rare and strong intensity earthquakes. Nonlinear deformations in cantilever walls ideally should occur in flexure in regions defined as plastic hinges. Traditionally, a single plastic hinge has been advocated inthe seismic design of each wall in these buildings (Paulay and Priestle 1992, CEN EC8 2004, NZS 3101 2006, ACI 318-08 2008). Codes include prescriptive requirements to ensure a certain degree of ductility in potential plastic hinge regions.

Some seismic design codes (EC8, NZS-3101, CSA) use Capacity Design to ensure elastic

[1]Graduate Student Researcher, Dept. of Civil and Environmental Engineering, University of California, Berkeley
[2]Assisstant Professor, Dept. of Civil and Environmental Engineering, University of California, Berkeley

response in regions other than the plastic hinges. To account for higher mode effects, these codes suggest a flexural design envelope which varies linearly from the expected flexural overstrength at the wall base to zero at the top. Recently, Panneton et al. (2006) ,Priestley et al. (2007), and Panagiotou and Restrepo (2009) have found that these provisions do not preclude the spread of plasticity into the upper regions. For buildings designed to develop a single plastic hinge at their base, near-fault ground motions can cause large demands along the height of the buildings due to concurrent first and second mode of response (Panagiotou and Restrepo 2009, Panagiotou et al. 2009). For this type of buildings has been shown that inelastic response at the base reduces mainly the contribution of the first mode of response (Rodriguez et al. 2002, Priestley et al. 2007, Panagiotou and Restrepo 2007). In this case the relative contribution of the second mode of response, relative to the first, increases with increasing nonlinearity.

Codes such as ACI 318-08 (2008) assume that plasticity concentrates at the base of the walls only (Wallace and Orakcal 2002). Because capacity design is not followed, plasticity can spread into regions above the wall's base under some circumstances (Yang et al. 2008, Panagiotou and Restrepo 2009). In these cases special detailing is required along the height of the wall to ensure that these regions can develop inelastic deformations.

Studies have proposed different design concepts for buildings, in which regions on the upper part of the structures are designed to accommodate significant deformations. Ziyaeifar and Noguchi (1996) proposed for shear-type buildings the use of a flexible isolation layer and a viscous damper, only on the upper part of the building. Panagiotou and Restrepo (2009) and Wiebe and Christopoulos (2009) proposed approaches where specific regions on the upper part of walls are designed to accommodate significant flexural deformations. The intention of these approaches is to reduce the contribution of the second and higher modes of response by allowing the structure to respond nonlinearly in these regions. Panagiotou and Restrepo (2009) proposed the design of a second flexural plastic hinge at mid-height of walls while Wiebe and Christopoulos (2009) proposed rocking of wall segments with respect to each other using unbonded post-tensioning.

This study investigates numerically the effectiveness of seismic isolation in tall buildings. The response of four 20-story cantilever wall buildings subjected to three near-fault ground motions is computed using nonlinear dynamic time history analysis. The first building, used as a reference, is designed to develop a single flexural plastic hinge at its base. The other three buildings are seismically isolated. Seismic isolation positioned at one or two locations along the height of the building allows significant shear deformations to concentrate at these locations.

Building Design and Computational Model

Four buildings are considered. Figure 1(a) shows the floor plan view of the four core wall buildings. Figure 1(b) shows the lateral seismic mass distribution, of the first building only, and an elevation view of the core wall of each of the four buildings. In all cases the lateral force resistance is assumed to be provided solely by a reinforced concrete core wall. It is also assumed that fifty percent of the gravity load is resisted by the core walls. The building height H, the floor height h, the seismic weight per floor w_i, as well as the main core-wall geometrical properties are

shown in Figures 1(a) and 1(b). Since it is assumed that all the lateral force resistance is provided by the core-walls from this point only the design and modeling of the core-walls is discussed.

The four buildings differ in the design of the locations, along the height of the walls, where nonlinear response can occur. The first building is designed to develop a flexural plastic hinge at its base only, while the other three buildings use lead-plug rubber bearing (LPRB) isolators (Naeim and Kelly 1999) at one or more locations along the height of the core walls. The first building, termed Single Plastic Hinge (SPH) and shown in Figure 1(b), is designed to concentrate all the plasticity at a single plastic hinge at the wall's base. The plastic hinge region extends to 10% of the building height and the reinforcing steel ratio in the plastic hinge region is equal to $\rho_{l,b}$ = 1.0%. Based on moment-curvature analysis the yield curvature of the wall φ_y and the expected flexural strength M_y at the base of the wall for an axial load P = 15360 kips are listed in Figure 1(c).

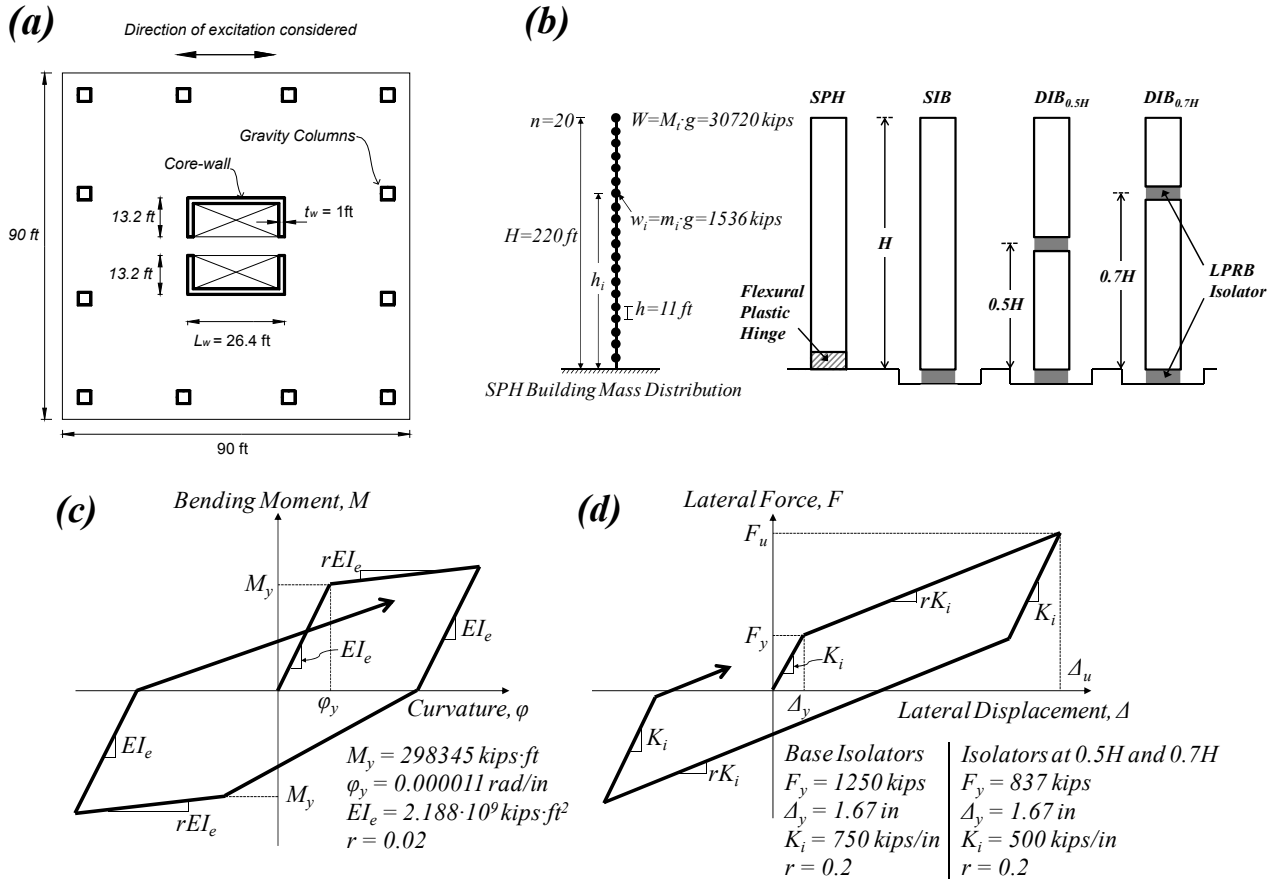

Figure 1. (a) Building floor plan, (b) mass distribution for SPH building and core walls' elevation, (c) flexural plastic hinge moment-curvature behavior, (d) seismic isolator force-displacement behavior.

The second building, shown in Figure 1(b), uses LPRB isolators only at its base and is termed Single Isolated Building (SIB). The third building uses LPRB both at its base and at mid-height and is termed Dual Isolated Building ($DIB_{0.5H}$). The fourth building uses LPRB isolators both at its base and at seventy percent of the height and is termed Dual Isolated Building ($DIB_{0.7H}$). The subscript 0.5H or 0.7H after the term DIB denotes the height where the second

layer of LPRB isolators is used in these buildings. The reasons for considering a second layer of isolation at 0.5H or 0.7H are explained in the section where the modal characteristics of the buildings are discussed.

Each layer of isolation assumes isolation of both the core walls and the gravity columns and uniform lateral deformation of all the isolators. Additionally the isolators are assumed to be rigid axially and any interaction between axial force, shear force and bending moment is ignored. It is noted that the axial flexibility of these isolators and its effect on the vertical dynamic characteristics of the structure may be important when vertical excitation is considered. From this point the isolation layer used at any elevation of the buildings is described with the bilinear-inelastic hysteretic behavior shown in Figure 1(d), where K_i is the initial stiffness, F_y the yield force, and r the post yield stiffness ratio. All the three isolated buildings have identical isolators at the base level. The $DIB_{0.5H}$ and $DIB_{0.7H}$ have identical isolators at 0.5H and 0.7H, respectively. The strength and stiffness characteristics of the isolators are given in Figure 1(d). The strength and the stiffness of the isolators at levels 0.5H and 0.7H are 67% of those of the base isolators. The isolation period based on the initial stiffness of the base isolator, defined as the period of the single degree of freedom system with mass equal to the total mass of the building and stiffness K_i is $T_b = 2\pi \sqrt{M_t / K_i} = 2.1\ sec$.

Because of the explanatory nature of the approach, simple nonlinear analytical tools and simple models are used in this investigation. For the SPH building all floors have identical lumped masses m_i. For the isolated buildings the mass is different, and equal to $1.5m_i$, at the floors where isolators exist. The core wall is modeled by one-component Giberson beam elements. The plastic hinge length at each of the two base elements is assumed to be half the element length. The hysteretic response in the plastic hinges is represented by the simple Clough hysteretic moment-curvature rule, see Figure 1(c) with a post-yield flexural rigidity ratio of r = 0.02. With the expected flexural strength M_y and the yield curvature φ_y, the flexural rigidity of the beam element is given by $EI_e = M_y / \varphi_y$. A limitation of the Giberson beam elements is that they do not consider the spread of plasticity caused by axial force – bending moment – shear force interaction in reinforced concrete. Consequently, curvatures obtained from the analyses should be taken as approximate only.

For the three isolated buildings the isolators are modeled as zero length nonlinear shear springs with the lateral force – lateral displacement behavior of Figure 1(d). The elastic portion of the walls in all the four buildings are modeled with elastic beam elements of flexural rigidity equal to $0.4EI_g$, where I_g is the gross section moment of inertia of the walls and E = 4000 ksi the elastic modulus of concrete. The models in this study ignore completely the tension stiffening effect which affects the initial period of the buildings and can also affect the response, especially in cases of limited nonlinear response or lightly reinforced walls. The effect of shear deformations is ignored too. The computer program Ruaumoko (Carr 1998) is used to estimate modal properties as well as to perform the nonlinear dynamic time history analyses (NDTHA). Large displacement theory is selected for the analyses and Caughey constant 2% viscous damping ratio is used in all the modes.

Ground Motions

Three strong near-fault earthquake records are considered in this study: the TAK0 record from the Mw 6.9 1995 Kobe earthquake, the LGP0 record from the Mw 6.9 1989 Loma Prieta earthquake and the RIN228 recorded from the Mw 6.7 1994 Northridge earthquake. Figure 2 plots the ground acceleration a_g time histories as well as the elastic acceleration and displacement spectra of the three records. All three records are characterized by large spectral displacements in the first mode period range, between 4.0 and 4.6 sec., as discussed below. The ground motions also result to large spectral accelerations and the displacements in the second modal period range of the buildings, between 0.6 and 1.4 sec., as will be also described below. The large spectral acceleration at these period ranges is due to the distinct acceleration pulses, in these ground motions, of duration in the period range of the second modal period of the buildings.

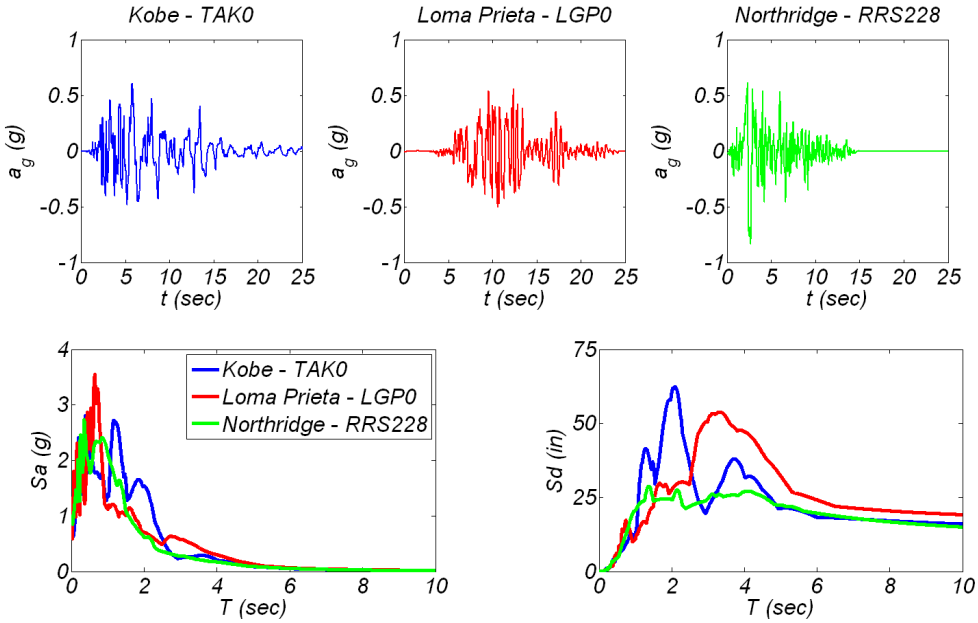

Figure 2. Ground motion time histories, acceleration and displacement response spectra, $\zeta = 2\%$.

Results of the Analyses

This section presents the main results of the modal analysis as well as of the NDTHA of the buildings subjected to the three ground motions. Modal analysis results are computed using initial stiffness properties of the buildings. Table 1 summarizes the first two modal periods of the buildings. The first mode period of the isolated buildings is 10 to 20% larger than the corresponding of the SPH building. Isolation has a more pronounced effect on the second modal period. The second modal period of the isolated buildings is more than two times this of the SPH building.

Figure 3 plots the normalized modal characteristics, based on initial stiffness properties, of the buildings: (a) lateral force, (b) bending moment, and (c) shear force diagrams of the first two modes. Modal lateral forces $F_{q,i}$ of mode q at floor i, are given as normalized by the product of the modal acceleration a_q of mode q times the seismic mass m_i at floor i. The normalized

modal forces are equal to the value of vector $\Gamma_q \Phi_q$ at floor i. Vector $\Gamma_q \Phi_q$ is the product of the modal participation factor Γ_q and the modal vector Φ_q. The modal bending moments $M_{q,i}$ are given normalized by the total seismic mass M_t times the height H of the building times a_q. Modal shear forces $V_{q,i}$ at floor i are given normalized by M_t times a_q. Figure 3 shows that based on the initial stiffness properties, isolation results in small differences in the first mode shape between the isolated and the SPH buildings. The effect of isolation is more pronounced on the second mode shape at the bottom half of the building. The differences between the modal characteristics of the two dual isolated buildings, $DIB_{0.5H}$ and $DIB_{0.7H}$ are small. Isolation increases the first and second normalized effective modal masses $V_{1,0} / M_t a_1$ and $V_{2,0} / M_t a_2$. Note that the sum of the normalized modal masses of the first two modes exceeds 0.99 in all the three isolated buildings while it is equal to 0.83 for the SPH building.

For the four buildings, the peak value of the second mode shear force above the building's midheight occurs at about 0.75H. For sign of second modal acceleration a_2 different than this of the first modal acceleration a_1 the modal shears of these modes have the same sign on the upper half of the buildings. In this case the height of peak shear force on the upper of the building depends on the relative amplitude of a_1 and a_2. Based on this observation the two heights of 0.5H and 0.7H are investigated as potential locations for the isolation layer.

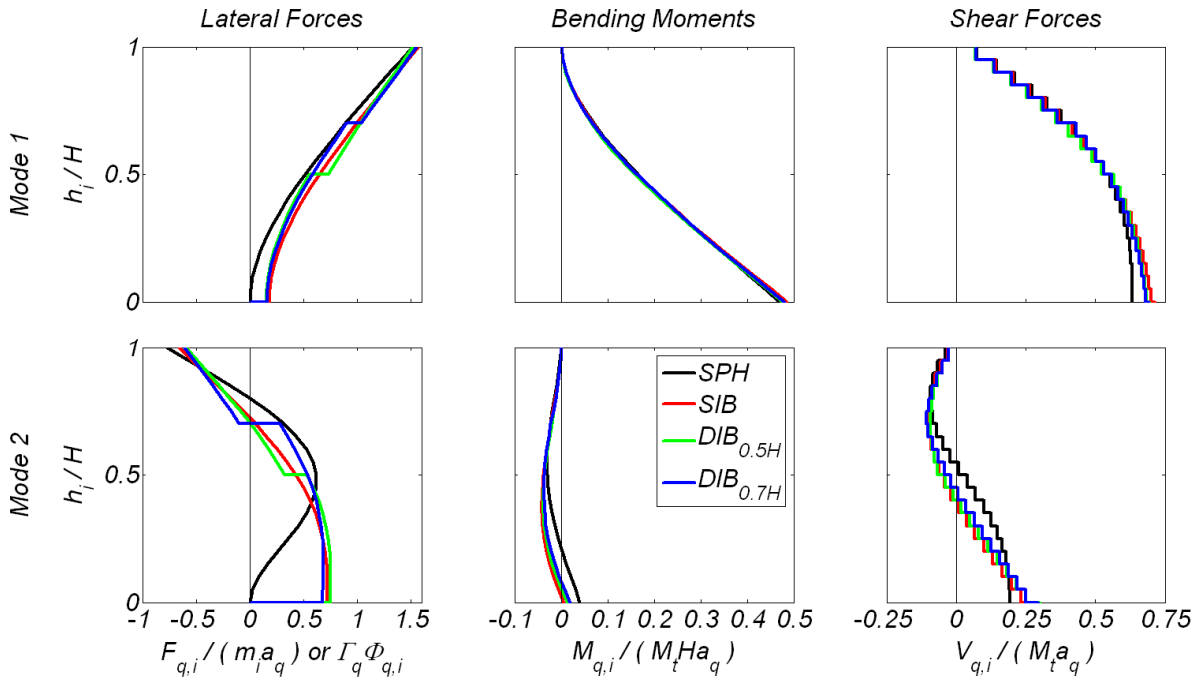

Figure 3. Modal characteristics of the buildings considered based on initial stiffness properties.

Table 1. Modal periods of the buildings considered.

	SPH	SIB	$DIB_{0.5H}$	$DIB_{0.7H}$
T_1 (sec)	4.0	4.3	4.6	4.5
T_2 (sec)	0.6	1.3	1.4	1.4

Figure 4 presents NDTHA response envelopes of the four buildings for the three near-fault ground motions. All the envelopes in the y axis plot normalized elevation height h_i to the building height H. Figure 4(a) plots peak relative displacements D_i and Figure 4(b) residual displacements. Figure 4(a) shows that for TAK0 and RRS228 records the isolated buildings result in smaller roof relative displacement, while for the LGP0 buildings SIB and $DIB_{0.7H}$ result in 8% and 22% larger roof displacement than the SPH building. Figure 4(b) shows that isolation significantly reduces residual displacements in comparison with the SPH building. This is due to the more origin-centered behavior that the LPRB force-displacement hysteresis experiences in comparison with the Clough behavior of the flexural plastic hinge region, especially for large deformations.

The SPH building experiences highly nonlinear response, especially for the LGP0 and the RRS228 records. The maximum computed curvature ductility, defined as $\mu_\varphi = \varphi_u / \varphi_y$ where φ_u is the maximum curvature and φ_y is the yield curvature, is equal to 3.5, 13.5, 14.1 for the TAK0, LGP0 and RRS228 records, respectively. Table 2 summarizes the maximum displacements of the isolators for buildings SIB, $DIB_{0.5H}$, and $DIB_{0.7H}$. All the isolators used at the base or on the upper part of the buildings result in displacements smaller than 21 in. The $DIB_{0.5H}$ and $DIB_{0.7H}$ buildings show similar isolator displacements both at the base and the upper part.

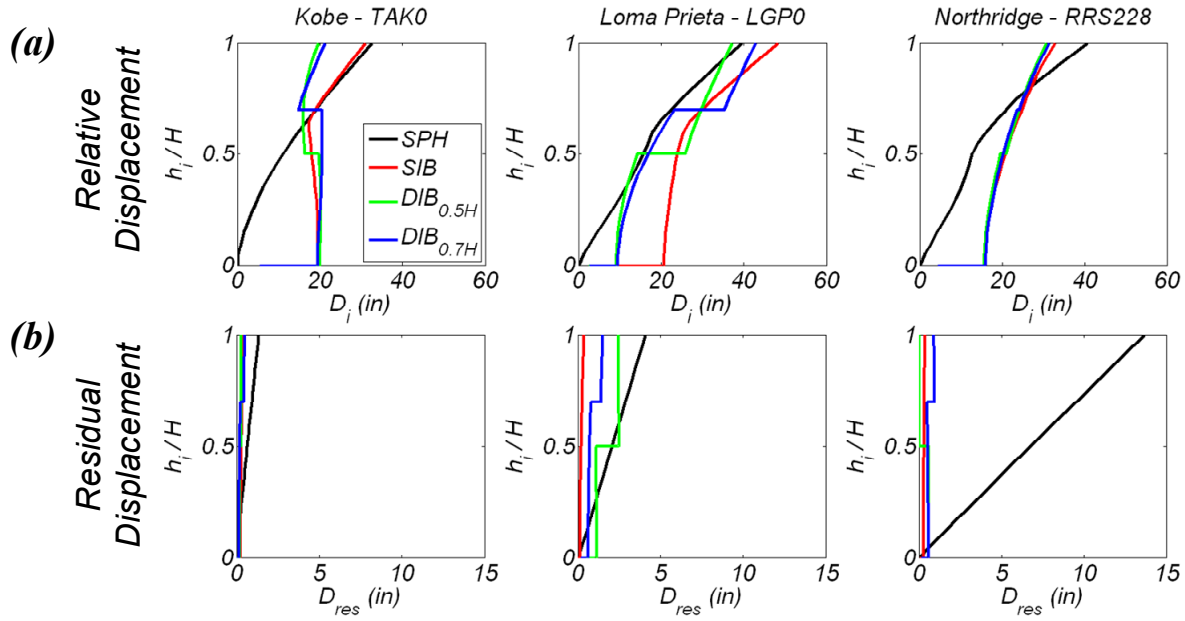

Figure 4. (a) Peak relative lateral displacement envelopes (b) Residual displacement envelopes.

Table 2. Max. isolator displacements and isolator residual displacements (in parenthesis) (in).

	SIB	**$DIB_{0.5H}$**		**$DIB_{0.7H}$**	
	Base Isolator	Base Isolator	Isolator at 0.5H	Base Isolator	Isolator at 0.7H
TAK0	19.6 (0.2)	20.0 (0.2)	10.8 (0.5)	19.4 (0.1)	12.0 (0.2)
LGP0	20.7 (0.1)	9.1 (1.1)	18.5 (1.4)	9.5 (0.6)	20.5 (0.6)
RRS228	15.8 (0.3)	15.6 (0.6)	12.8 (0.6)	16.0 (0.6)	14.4 (0.4)

Figures 5(a), (b) and (c) plot the shear force, bending moment, and floor absolute acceleration envelopes, respectively. Shear forces V_i at floor i are given normalized by the total seismic weight W of the buildings. Floor absolute accelerations A_i are given normalized by the peak ground acceleration PGA. Figure 5(a) clearly shows that the isolated buildings result in significant reduction of shear forces along the height of the buildings in comparison with the SPH building. The reduction of the base shear for the isolated buildings in comparison with the SPH building ranges between 60% and 80%. The isolated buildings result in similar base forces while the dual isolated buildings develop smaller shear forces on the upper 60% of the height of the buildings. This is because the second layer of isolation placed at 0.5H or 0.7H effectively reduces the maximum shear force that can be developed on the upper part of the building.

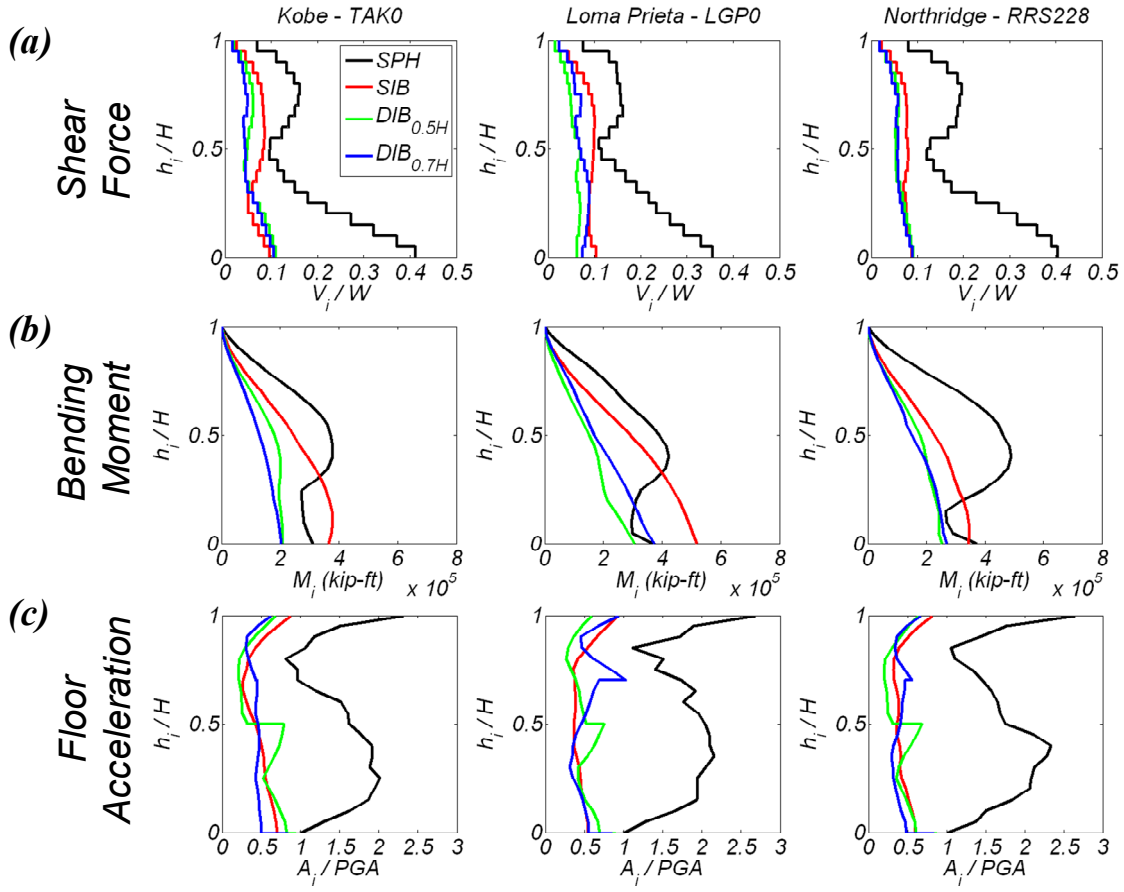

Figure 5. (a) Shear force, (b) Bending moment, (c) Floor absolute acceleration envelopes.

Figure 5(b) shows that isolation results also in significant reduction of the bending moment along the height of the buildings for all the three records. It is noted that for the SPH building the bending moment close to midheight is larger than the bending moment at the base of the structures. In order the wall to remain elastic for this bending moment demand, the required longitudinal steel ratio is large to excessive. For the RRS228 motion the required longitudinal steel ratio is equal to 3.65%. This is due to the large bending moments at these locations in combination with the reduced axial load in the wall. The DIBs show smaller bending moments

along their heights in comparison with the SIB. This is because the second isolation layer on the upper part of the building further reduces the shear force that can be transmitted at the lower part of the walls.

Lastly, Figure 5(c) shows the effectiveness of isolation on the floor absolute accelerations. In comparison with the SPH building the seismic isolated buildings result in significant reduction, 30% to 80%, of the floor accelerations along the height. It is noted that for the SPH building, although the highly inelastic response at the base, floor accelerations are nearly greater than the peak ground acceleration along all the height of the buildings for all the three motions. This observation agrees with previous analytical and experimental studies (Rodriguez et al. 2002, Panagiotou and Restrepo 2009, Panagiotou et al. 2009). The three isolated buildings demonstrate the same level of effectiveness in reducing floor accelerations in comparison with the SPH building.

Conclusions

This paper studied numerically the response of four 20-story cantilever reinforced concrete wall buildings, three of which used LPRB isolators, subjected to three strong near-fault ground motions. The four buildings differ in terms of the locations where nonlinear response could develop in the wall. The first building is designed to develop a single plastic hinge (SPH) at the base of the wall. The second had seismic isolators at its base. The third had seismic isolators at its base and at midheight, while the fourth had seismic isolators at its base and at seventy percent of the height. Nonlinear dynamic time history analysis of these buildings is carried. The investigation led to the following conclusions:

1. Near fault ground motions with large first and second mode spectral accelerations and displacements cause significant displacement, force and acceleration demands in tall cantilever wall buildings.

2. The isolated buildings demonstrate a significant reduction in all engineering response quantities considered, in comparison with the SPH building. The reduction in shear forces, bending moments at midheight, and floor accelerations is more than 50% in all cases. The isolated buildings also resulted in more than 80% reduction of the residual displacements due to the relatively origin-centered hysteretic behavior of the isolators.

3. The single and dual isolated buildings have similar response in terms of maximum base shear force and floor accelerations. The dual isolated buildings resulted in smaller bending moment along the height of the walls and shear forces on the upper 60% of the walls' height. The reduction in both quantities is by up to a factor of two.

4. For the SPH building significant inelastic response and curvature ductility demand is computed at the base of the walls. In spite of the highly nonlinear response of the wall, large shear forces, bending moments, and floor accelerations are developed along its height. For the case of RRS228 record the SPH building's response ended with excessive residual displacements.

References

ACI 318-08, 2008. *Building Code Requirements for Structural Concrete (ACI 318-08) and Commentary*. ACI Committee 318, Farmington Hills.

Carr, A.J., 1998. *Ruaumoko – A Program for Inelastic Time-History Analysis*. Department of Civil Engineering, University of Canterbury, New Zealand.

CEN EC8, 2004. *Design of Structures for Earthquake Resistance.* European Committee for Standardisation, Brussels, Belgium.

CSA Standard A23.3-04., 2005. *Design of Concrete Structures*. Canadian Standard Association, Rexdale, Canada. p.214.

Krishnan, S., 2007. Case Studies of Damage to 19-storey Irregular Steel Moment-Frame Buildings under Near-Source Ground Motion. *Earthquake Engineering and Structural Dynamics* 36, 861-885.

Naeim, F., Kelly, J.M., 1999. *Design of Seismic Isolated Structures: From Theory to Practice*. Wiley & Sons, New York City.

NZS 3101., 2006. *New Zealand Standard, Part 1- The Design of Concrete Structures, Standards New Zealand*. Wellington, New Zealand.

Panagiotou, M., Restrepo, J.I., 2007. Lessons Learnt from the UCSD Full-scale Shake Table Testing on a 7-Story Residential Building Slice. *Proceedings SEAOC Convention*, 57-73.

Panagiotou, M., Restrepo, J.I., 2009. Dual-Plastic Hinge Design Concept for Reducing Higher-Mode Effects on High-Rise Cantilever Wall Buildings. *Earthquake Engineering and Structural Dynamics*, February online edition.

Panagiotou, M., Calugaru, V., Visnjic, T., 2009. Higher Mode Effects on the Seismic Response of Tall Cantilever Wall Buildings Subjected to Near Fault Ground Motions. *Proceedings SEAOC 2009 Convention, San Diego, CA*, 345-357.

Panneton, M., Léger, P., Tremblay, R., 2006. Inelastic Analysis of a Reinforced Concrete Shear Wall Building According to the National Building Code of Canada 2005. *Canadian Journal of Civil Engineering* 33, 854-871.

Paulay, T., Priestley, M.J.N., 1992. *Seismic Design of Reinforced Concrete and Masonry Buildings*. John Wiley & Sons, Inc., Hoboken, NJ.

Priestley, M.J.N., Calvi, G.M., Kowalsky, M.J., 2007. *Displacement Based Seismic Design of Structures*. IUSS Press, Pavia, Italy.

Rodríguez, M.E., Restrepo, J.I., Carr, A.J., 2002. Earthquake-Induced Floor Horizontal Accelerations in Buildings. *Earthquake Engineering and Structural Dynamics* 31, 693-718.

SEAONC, 2007. *SEAONC Recommended Administrative Bulletin for San Francisco.* Structural Engineers Association of Northern California, San Francisco.

Wallace, J.W., Orakcal, K., 2002. ACI 318-99 Provisions for Seismic Design of Structural Walls. *ACI Structural Journal* 99 (4), 499-508.

Wiebe, L., Christopoulos, C., 2009. Mitigation of Higher Mode Effects in Base-Rocking Systems by Using Multiple Rocking Sections. *Journal of Earthquake Engineering* 13 (1), 83–108.

Yang, T.Y., Bozorgnia, Y., Moehle, J., 2008. The Tall Buildings Initiative. *Proceedings 14th World Conference on Earthquake Eangineering, Beijing, China*.

Ziyaeifar, M., Noguchi, H., 1998. Partial Mass Isolation in Tall Buildings. *Earthquake Engineering and Structural Dynamics* 27 (1), 49-65.